

Composition of the L5 Mars Trojans: Neighbors, not siblings

Andrew S. Rivkin^{a,*,1}, David E. Trilling^b, Cristina A. Thomas^{c,1}, Francesca DeMeo^c,
Timothy B. Spahr^d, Richard P. Binzel^{c,1}

^a *Johns Hopkins University Applied Physics Laboratory, 11100 Johns Hopkins Rd., Laurel, MD 20723, USA*

^b *Steward Observatory, The University of Arizona, Tucson, AZ 85721, USA*

^c *Department of Earth, Atmospheric, and Planetary Sciences, Massachusetts Institute of Technology, Cambridge, MA 02139, USA*

^d *Harvard-Smithsonian Center for Astrophysics, 60 Garden St., Cambridge, MA 02138, USA*

Received 24 April 2007; revised 26 June 2007

Available online 11 September 2007

Abstract

Mars is the only terrestrial planet known to have Trojan (co-orbiting) asteroids, with a confirmed population of at least 4 objects. The origin of these objects is not known; while several have orbits that are stable on Solar System timescales, work by Rivkin et al. [Rivkin, A.S., Binzel, R.P., Howell, E.S., Bus, S.J., Grier, J.A., 2003. *Icarus* 165, 349–354] showed they have compositions that suggest separate origins from one another. We have obtained infrared (0.8–2.5 μm) spectroscopy of the two largest L5 Mars Trojans, and confirm and extend the results of Rivkin et al. We suggest that the differentiated angrite meteorites are good spectral analogs for 5261 Eureka, the largest Mars Trojan. Meteorite analogs for 101429 1998 VF31 are more varied and include primitive achondrites and mesosiderites.

© 2007 Elsevier Inc. All rights reserved.

Keywords: Asteroids; Asteroids, composition; Trojan asteroids

1. Introduction

Mars is the only terrestrial planet known to have co-orbiting “Trojan” asteroids. These objects reside in stability zones centered on the Lagrangian points 60° leading and trailing the planet. Jupiter and Neptune also have Trojan asteroid companions, with the population associated with Jupiter estimated to number roughly 160,000 with radii larger than 1 km in the L4 cloud. By contrast, Mars’ known retinue is considerably more modest. Unlike Jupiter Trojans, the definition of a Mars Trojan is not clear-cut, with long-term integrations necessary to establish the stability of a candidate’s orbit. At this writing, there are four confirmed objects (listed below) and a handful of other

suspects (including 2001 FR127) identified by the Minor Planet Center. All but one of these objects trail Mars.

The set of stable orbits near Mars has been studied by Tabachnik and Evans (1999) and Scholl et al. (2005), who found that 5261 Eureka, 101429 1998 VF31, 121514 1999 UJ7, and 2001 DH47 are in areas that are stable on timescales longer than the age of the Solar System, consistent with an origin in their current orbits. However, Rivkin et al. (2003) found the visible spectrum of 1999 UJ7 to be significantly different from that of Eureka and 1998 VF31, and that these objects were unlikely to have all formed at the same solar distance. The visible spectra and limited infrared spectrophotometry suggested an Sa- or A-class membership for Eureka and 1998 VF31, and an X-class membership for 1999 UJ7. Eureka is currently the largest known Mars Trojan, with a diameter of roughly 1.3 km, while the diameter of 1998 VF31 is slightly less than 800 m (Trilling et al., 2007). A detailed discussion of the dynamics of Mars Trojans can be found in Scholl et al. (2005) and Connors et al. (2005), and for Trojans in general in Marzari et al. (2002), but is beyond the scope of this paper.

* Corresponding author.

E-mail address: andy.rivkin@jhuapl.edu (A.S. Rivkin).

¹ Visiting Astronomer at the Infrared Telescope Facility, which is operated by the University of Hawaii under Cooperative Agreement No. NCC 5-538 with the National Aeronautics and Space Administration, Science Mission Directorate, Planetary Astronomy Program.

Table 1
Observing circumstances for Mars Trojans

Object	Date	Observers	V mag	Phase angle	Standard stars
5261 Eureka	11 May 2005	Binzel and Thomas	16.4	11.3°	L102, L105, L110
	19 May 2005	Rivkin	16.0	4.5°	L102, L105
101429 1998 VF31	10 May 2005	Binzel and Thomas	18.0	26.2°	L102, L110

Note. Codes for standard stars are as follows: L102 = L102–1081, L105 = L105–56, L110 = L110–361, where all are from the Landolt (1983) catalog. The V magnitudes for the asteroids were taken from the JPL Horizons ephemeris.

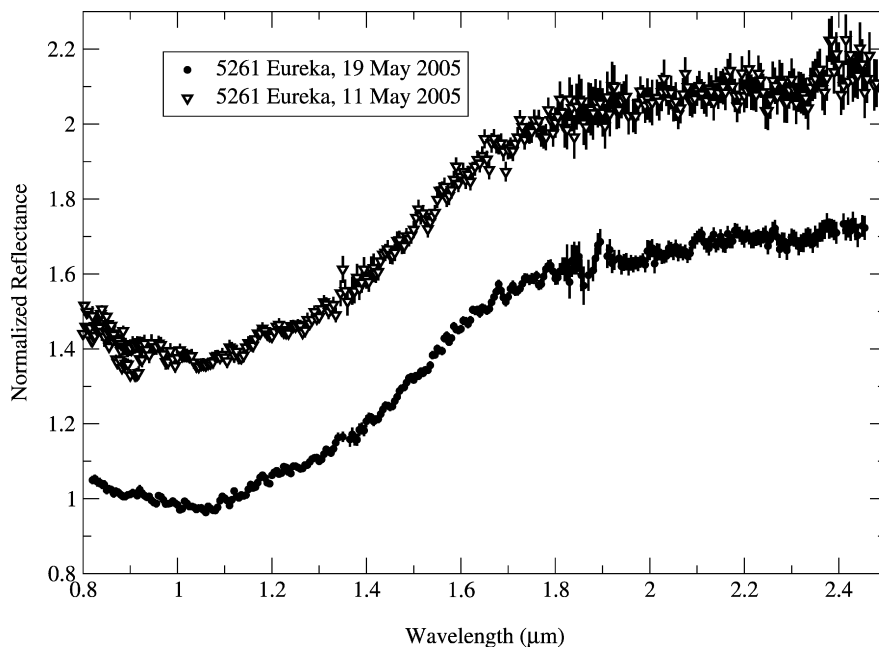


Fig. 1. Two spectra of Eureka taken with SpeX at the IRTF, from 11 and 19 May 2005. The agreement between these spectra are excellent, both showing a broad, deep 1- μm absorption and a relatively straight, flat spectrum beyond $\sim 1.8 \mu\text{m}$. The spectra are normalized to 1 at 1 μm , and the 11 May spectrum was offset from the 19 May spectrum for clarity. The structure near 1.9 μm in the bottom spectrum is interpreted as noise rather than having mineralogical significance.

2. Observations

Spectroscopic data were obtained using SpeX on the Infrared Telescope Facility (IRTF) on Mauna Kea, Hawaii (Rayner et al., 2003). The instrument was in “prism mode,” which provides continuous coverage over the 0.8–2.5 μm spectral range with a resolution of 250. Standard stars taken from the Landolt (1983) catalog and extensively observed by Bus and Binzel (2002) were observed several times over the course of the nights and are included in Table 1. The data reduction was performed using a combination of IRAF (Tody, 1986) and IDL routines to first extract the asteroid and standard spectra, wavelength-calibrate the spectra, and finally to remove any residual telluric contamination. A more detailed description of the data reduction steps is provided in Rivkin et al. (2004). The Asteroid 5261 Eureka was observed on two nights, 1998 VF31 on one. The observing circumstances for each object are shown in Table 1.

The spectra of silicates have been shown to be temperature dependent in the wavelength region studied in this work (Singer and Roush, 1985; Hinrichs and Lucey, 2002; Moroz et al., 2000), potentially complicating comparisons to room-temperature laboratory spectra. The objects presented in this work, however, have surface temperatures near 250 K (Trilling

et al., 2007). Therefore, these corrections are not important for Eureka and 1998 VF31 and in this case can be safely neglected.

3. Results

3.1. 5261 Eureka

There is excellent agreement between the two Eureka spectra, as shown in Fig. 1. Because the 19 May spectrum is of higher quality than the 11 May spectrum (as expected since Eureka was brighter on that date), it alone will be shown in later figures. However, given the agreement between these spectra, all conclusions reached are consistent with the first spectrum as well.

The spectrum of Eureka shows a broad, deep absorption band centered near 1.08 μm , with no obvious corresponding 2- μm band. This is interpreted as evidence for olivine, with little if any iron-bearing pyroxene present. The visible-region spectra of Eureka from Rivkin et al. (2003) can be used to construct a full 0.4–2.5 μm spectrum, from which commonly used spectral parameters can be extracted (see Cloutis et al., 1986, for instance).

S-class and related asteroids are often interpreted using Band Area Ratio (BAR)/Band I plots, popularized by Gaffey et al.

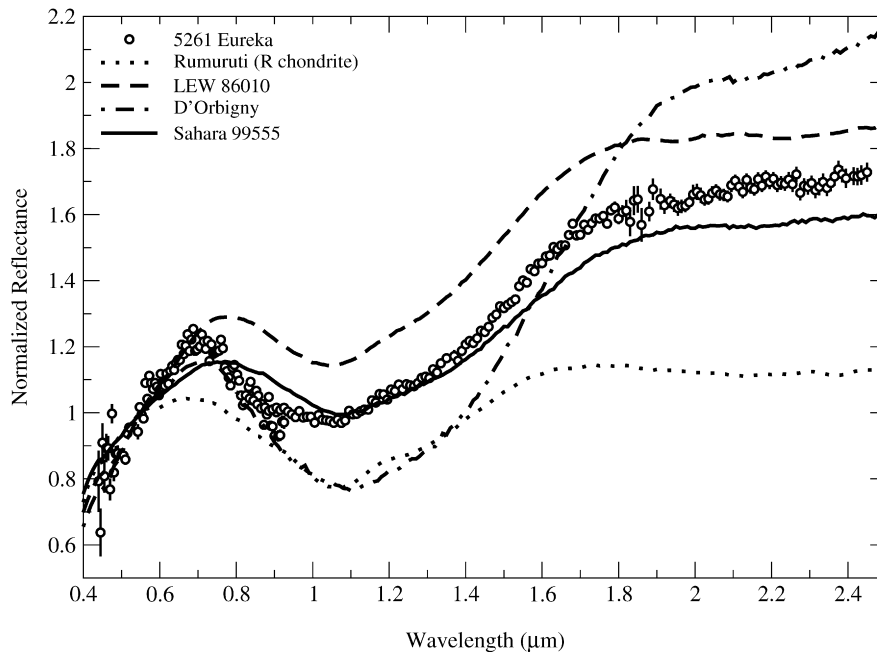


Fig. 2. Eureka compared to angrite meteorites, and also to the R chondrite Rumuruti. The angrites bracket Eureka's spectrum well. While Rumuruti is the only R chondrite for which a spectrum is available, it does not obviously match Eureka, failing to match its overall spectral slope. However, additional spectra for additional R chondrites are necessary to fully reject them as analogs for Eureka.

(1993). In these plots, a subclassification within the S class can be made using the position of the 1- μm band center and the ratio of the areas of the 1- and 2- μm bands. That subclassification can give an idea of the relative proportions of olivine and pyroxene on an object's surface as well as identifying potential analogs among the known or a hypothesized meteorite population.

As can be seen from Fig. 1 and as mentioned above, there is no evidence for a resolvable 2- μm band on Eureka, leading to a BAR ~ 0 . Its Band I position is 1.08 ± 0.02 . Together, these lead to a classification in the S(I) subclass. Gaffey et al. (1993) suggest that these objects are consistent with olivine-metal mixtures, possibly analogous to pallasite meteorites.

Burbine et al. (2006) measured reflectance spectra for 3 angrites and found them to have properties similar to what we find for Eureka: broad absorption bands near 1 μm and weak or absent 2- μm bands, which would also be classified as S(I) in the Gaffey et al. (1993) scheme. Fig. 2 shows Eureka's spectrum compared to the angrite spectra from Burbine et al. (2006). The asteroid fits well among the others, particularly LEW 86010 and Sahara 99555, and is bracketed by the diversity shown in the meteorite spectra.

The angrite meteorites are igneous, generally basaltic rocks that have unusual mineralogies including anorthosite, Ca-rich olivine, and Ca–Al–Ti-rich pyroxenes. Their oxygen isotopes are similar to some other groups, including the HEDs and mesosiderites, but their peculiar mineralogies and compositions suggest they are unrelated to those groups (Weisberg et al., 2006). Geochemical studies suggest that the angrites are the igneous products of carbonaceous chondrites, though other origins have also been proposed (Kurat et al., 2004; Varela et al., 2005).

We modeled the reflectance spectrum of Eureka using angrites and a neutral component to see if an acceptable fit could be achieved using only those components. The results are shown in Fig. 3. We used a Hapke bi-directional scattering model to mix end-member mineral spectra to simulate our whole-disk observations of Eureka. Using software developed for analysis of NEAR Shoemaker spectra of Asteroid 433 Eros (Clark et al., 2002b, 2004), we simulated intimate mixtures of a set of 5 end-member spectra. Our end-members were the angrites D'Orbigny, Sahara 99555, and LEW 86010, and neutral phase spectra with albedos varying from 0.1 to 0.6. Spectrally neutral phases have been necessary in all spectral modeling of airless rocky planetary surfaces to represent low-albedo and/or non-crystalline components. End-member spectra were obtained from T. Burbine for the angrites, or constructed for the neutral phases. End-members were measured at grain sizes of less than 125 μm (D'Orbigny and Sahara 99555) or less than 74 μm (LEW 86010). Our mixture model simulations are not meant to indicate unique determinations of composition. However, if the assumption is made that the end-member choices are accurate, such models can be used as indicators of relative proportions of detected components.

The asteroid spectra were modeled including albedo/reflectance information. For the models, Eureka's albedo was set to 0.39 or 0.26 representing nominal and 1- σ low values of its measured albedo. The determination of the radiometric albedos of Eureka and 1998 VF31 is presented in a companion paper (Trilling et al., 2007). These albedo values are consistent with the spectral class found for Eureka, particularly NEOs of similar size observed by Delbó et al. (2003). As seen in Fig. 3, Eureka's spectrum can be fit quite well with only angritic

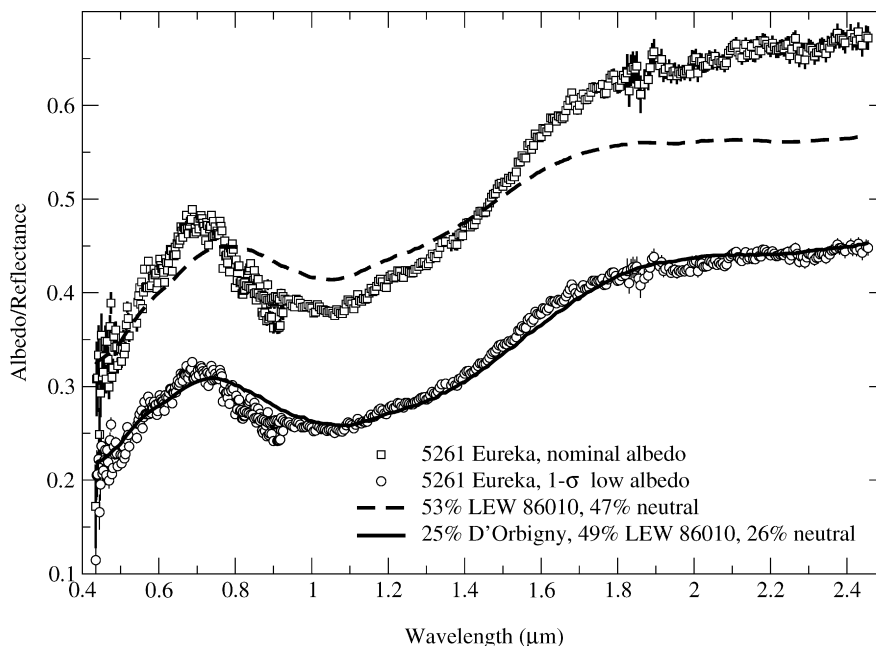


Fig. 3. Mixture modeling fits for Eureka. These fits were calculated using only the Angrites from the previous figure and flat (neutral) spectra as end-members. Two cases were modeled, one with an albedo of 0.39 for Eureka, the other 0.26. These values match the mean and $1-\sigma$ low values for Eureka's albedo, measured by Trilling et al. (2007). The match is very good in particular for the lower-albedo case, and no other components are obviously necessary to provide an acceptable match.

and neutral components when using the $1-\sigma$ low value for its albedo. That fit includes 49% LEW 86010, with D'Orbigny contributing roughly half as much to the spectrum and the neutral component (with albedo of 0.6) making up the remainder of the model fit components. Although not a unique fit, this excellent fit strongly supports an Angritic interpretation for Eureka. For the nominal albedo case, the fraction of the high albedo neutral component must increase, and does so at the expense of D'Orbigny, the lower-reflectance Angrite. The fit is poorer than the low-albedo case. The $1-\sigma$ high albedo for Eureka does not result in an acceptable fit, and is not shown.

Another possible match is also shown in Fig. 2. Eureka qualitatively matches a spectrum of Rumuruti powder (Burbine et al., 2002; Sunshine et al., 2005), a member of the rare R chondrite class, and the only known fall of that type. R chondrites are relatively oxidized, anhydrous, metal poor, primitive meteorites with high olivine fayalite contents (McSween et al., 2006). They are thought to have formed at greater heliocentric distances than the ordinary chondrites (Kallemyn et al., 1996). In this interpretation, Eureka would be undifferentiated. However, we prefer the Angrite interpretation for Eureka for two reasons: first, the match to Eureka in the blue and ultraviolet region is better for the Angrite spectra than for Rumuruti. Second, spectra of Rumuruti vary considerably, with those of saw-cut surfaces showing blue spectral slopes for two of the three lithologies measured and a too-low albedo for the third lithology (Berlin et al., 2003). We note that spectra from these saw-cut surfaces may not be a good representation of the spectra one would receive from an asteroidal surface. Additional spectra of Rumuruti and other R chondrites may strengthen or weaken an R-chondrite interpretation of Eureka with respect to possible meteorite parent bodies. However, at this time we can-

not formally rule out a connection between Eureka and the R chondrites.

3.2. 101429 1998 VF31

The Asteroid 1998 VF31 has a visible and near-IR spectrum typical of S-class asteroids (Fig. 4). Although the data are rather noisier than the Eureka spectrum, we can still determine the band parameters, with a band center of 0.9 ± 0.03 and a BAR of 2.0 ± 0.3 . While not as precise as might be desired, this is still sufficient to firmly place 1998 VF31 into the S(VII) subclass. Fig. 4 includes two bright S(VII) asteroids (40 Harmonia and 57 Mnemosyne) for which high-quality SMASS and SpeX data are available, showing a similarity that supports such a classification for 1998 VF31.

In Rivkin et al. (2003), 1998 VF31 was interpreted as an Sr-, Sa-, or A-class object based on its similarity to the spectrum of Eureka over the limited visible wavelengths that it was observed. With the benefit of much-expanded wavelength coverage and a near-IR spectrum of higher quality than the visible spectrum previously available, it is clear that 1998 VF31 is quite different from Eureka beyond $0.8 \mu\text{m}$. Its spectrum shows both 1- and $2-\mu\text{m}$ bands, typical of S-class asteroids.

An upturn in flux beyond $2.1 \mu\text{m}$ for 1998 VF31 is reminiscent of thermal emission seen in some near-Earth objects. While the surface temperatures of Mars Trojans are warmer than their main-belt cousins, the albedo required for detectable thermal emission near $2.4\text{--}2.5 \mu\text{m}$ at 1998 VF31's solar distance is unrealistically low (~ 0.04 or less) given what is usually seen for S-class asteroids and would conflict with the value of ~ 0.32 measured by Trilling et al. (2007). Therefore, we interpret the upturn as a part of a general spectral slope on the object.

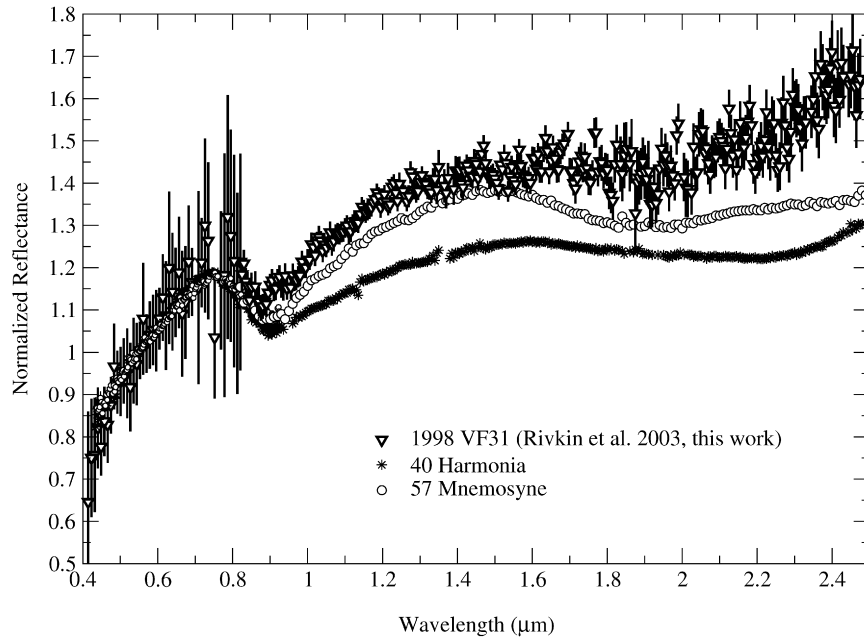


Fig. 4. Spectrum of 1998 VF31 compared to two S-class asteroids. All are classified as S(VII) objects in the Gaffey et al. (1993) subclassification scheme. The spectral slope for 1998 VF31 is higher than for either main-belt asteroid, but the overall spectral characteristics are qualitative matches. The rise in reflectance for 1998 VF31 beyond $\sim 2.2 \mu\text{m}$ is not due to thermal emission, and can be seen in 40 Harmonia, as well.

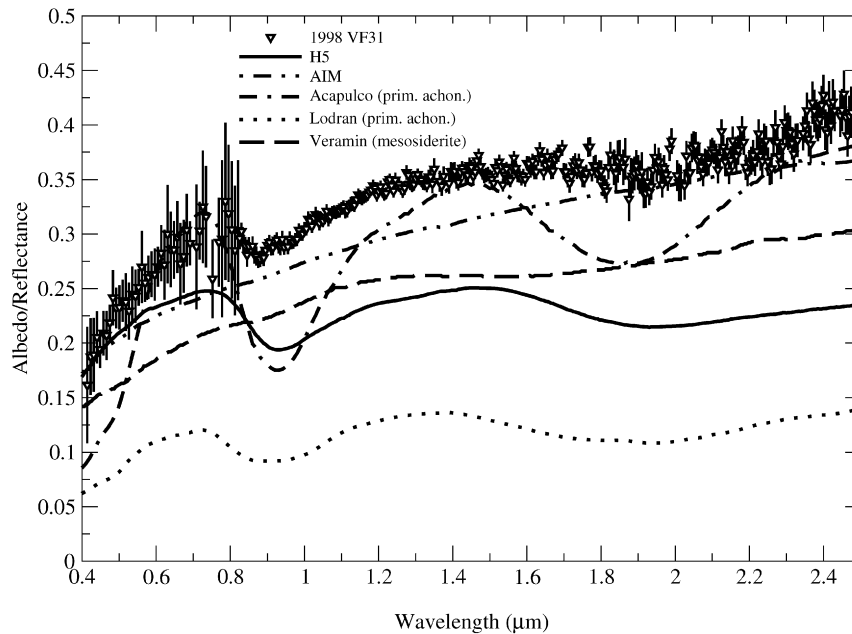


Fig. 5. End-members used in mixing models for 1998 VF31. The mesosiderite Veramin, the average spectra for H5 meteorites and iron meteorites (AIM in the figure) were used from Gaffey (1976). The primitive achondrite spectra were obtained from RELAB. The spectrum of 1998 VF31 is also included, scaled to the nominal measured albedo from Trilling et al. (2007). Primitive achondrites and mesosiderites are possible analogs for S(VII) asteroids according to Gaffey et al. (1993). Ordinary chondrites were also included in the mixing models, though only H chondrites had a contribution to the fit. All of these meteorite spectra are of lower albedo than the asteroid, as with Eureka.

Interestingly, the much larger main-belt Asteroid 40 Harmonia also has an upturn at longer wavelengths, as seen in Fig. 4.

The S(VII) asteroids are interpreted by Gaffey et al. (1993) as possibly analogous to any of a variety of primitive achondrites, or possibly mesosiderites, though they found that interpretation unlikely. Heating of a chondritic precursor in the presence of a reducing agent was also proposed as a possibility.

As with Eureka, mixing models were performed for 1998 VF31, using the primitive achondrites Acapulco and Lodran, the mesosiderite Veramin, the average of the iron meteorites (AIM) in Gaffey (1976), and a neutral component. The meteorite end-members are shown in Fig. 5. The larger uncertainties in 1998 VF31's spectrum, as well as a smaller selection of suitable end-member spectra, leave this fit somewhat less certain

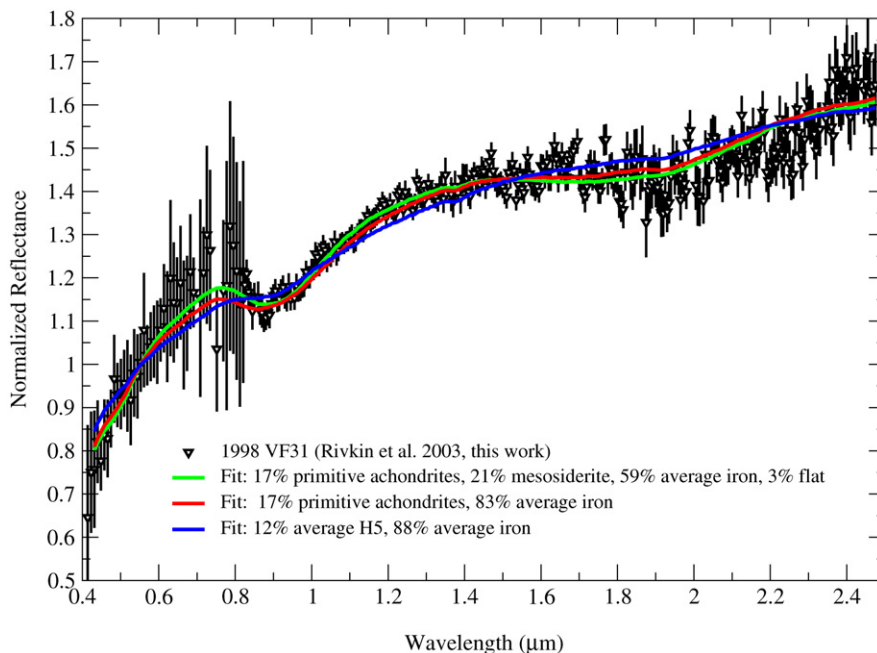


Fig. 6. Mixture models for 1998 VF31. Although the spectrum for 1998 VF31 is noisier than for Eureka, the mixture model is still instructive. The model assemblage is dominated by iron, with roughly 17% primitive achondrite. Models with ordinary chondrite end-members are even more dominated by iron, and do not produce as good a fit. All of these model fits have albedos of roughly 0.2, consistent with the $1-\sigma$ low albedo of 1998 VF31 from Trilling et al. (2007).

than the fit for Eureka. As shown in Fig. 6, the model spectra are dominated by metal, with roughly 80% of the contribution coming from a combination of the AIM and Veramin spectra, with the remaining 20% contribution from a combination of the primitive achondrites. A fit using only H5 chondrite ($\sim 12\%$, also shown in Fig. 6) and AIM ($\sim 88\%$) spectra is also consistent, though is of much lower quality. All of these fits give an albedo of roughly 0.2, again lower than the nominal radiometric albedo of $0.32^{+0.18}_{-0.11}$ in Trilling et al. (2007) but consistent within observational uncertainties. It is conceivable that the large metal fraction indicated by these fits is a sign that the surface of 1998 VF31 has undergone regolith maturation (aka space weathering: Clark et al., 2002a, and others), but we might expect little regolith on an asteroid of this size. A more thorough consideration of space weathering and 1998 VF31 is beyond the scope of this work. However, we conclude that 1998 VF31's spectrum is most consistent with a mixture of metal and primitive achondrites, either with or without mesosiderite contribution.

4. The origin of the Mars Trojans

The visible spectra of three Mars Trojans were interpreted by Rivkin et al. (2003) as showing that they all could not have formed at their current distances, though the two objects at L5 (Eureka and 1998 VF31) could be related. With expanded wavelength coverage and the most likely mineralogical interpretations presented above, it appears unlikely that the L5 objects are related to one another. An angritic composition for Eureka suggests an oxidized, carbonaceous chondritic precursor. If Eureka is more like Rumuruti and the R chondrites, it would again be expected to be more oxidized than the ordi-

nary chondrites. 1998 VF31, if a primitive achondrite, would be expected to have originated on reduced objects relative to ordinary chondrites. Furthermore, all of the suggested analogs for S(VII) objects have significantly different oxygen isotopes than angrites or the R chondrites, again indicating a different parent body (or, of course, that we do not have samples of the relevant objects). The most straightforward explanation is that Eureka and 1998 VF31 are not related, and presumably at least one (if not both) were captured into their current orbits at some point in Solar System history, perhaps very early. We also note for completeness that Phobos and Deimos have spectra very different from the L5 objects, suggestive of outer-belt asteroids or mature lunar soils (Rivkin et al., 2002; Gendrin et al., 2005), as discussed further in Rivkin et al. (2003).

New dynamical models have been proposed in recent years that suggest a large flux of objects were scattered from the asteroid belt and Kuiper belt roughly 4 byr ago (Gomes et al., 2005). It has been proposed that during this period, the Trojan asteroids of Jupiter were captured into their current orbits (Morbidelli et al., 2005). Morbidelli (private communication; also reported in Scholl et al., 2005) suggested that the capture of Mars Trojans could be aided by a chaotic wandering of Mars' semi-major axis due to impacts between proto-Mars and lunar-size planetary embryos.

The igneous events that formed the angrites occurred very early in Solar System history, allowing plenty of time for collisions to break up the angrite parent body and then allow at least one piece to be captured as a Mars Trojan. Argon dating of R chondrites by Dixon et al. (2003) suggests early impact events on that parent body, again creating the opportunity for ejecta to be created and captured into Mars Trojan orbits.

Given the much larger set of possible compositions for 1998 VF31, its story is less easy to pin down. Mesosiderites are thought to have had a major degassing event roughly 3.9 byr ago, interpreted as collisional disruption (Rubin and Mittlefehldt, 1993) and consistent with capture by Mars at that time. This is also the same era as the late heavy bombardment. Primitive achondrites are thought to have been heated early in Solar System history, as well.

Taking the spectroscopic, meteoritic, and dynamical evidence all together, the simplest explanation for the origins of Eureka and 1998 VF31 is that they formed separately in other parts of the inner Solar System as part of larger bodies, those bodies were disrupted during the earliest times in the Solar System and pieces found themselves trapped in the 1:1 resonance with Mars by roughly 3.9 byr ago. Thus, they are most likely to be long-term residents but not natives. Additional work will be necessary to determine the total population of the neighborhood and whether all of the inhabitants are immigrants.

Acknowledgments

The data taken here were obtained through the SMASS and MIT-IRTF-UH surveys as targets of opportunity. This work was supported by NASA Planetary Geology and Geophysics Grant NNG06GA23G. As usual, Dave, Bill, Paul, and Eric at the IRTF were indispensable to actually getting the data in the first place. Data from RELAB were critical for our analysis, and we thank Tom Burbine for sharing his meteorite spectra. Helpful reviews by Tom Burbine and Sonia Fornasier improved and strengthened this manuscript. This work has made use of NASA's Astrophysics Data System. Thanks to Gwen Bart, Ross Beyer, Dave O'Brien, and Paul Withers for creating the L^AT_EX template used for this manuscript. And continuing thanks to the indigenous people of Hawai'i for allowing astronomers to use their sacred mountain.

References

- Berlin, J., Lingemann, C.M., Stöffler, D., 2003. Visible and near-infrared reflectance spectra of Rumuruti. *Lunar Planet. Sci.* 34. Abstract 1764.
- Burbine, T.H., McCoy, T.J., Hinrichs, J.L., Lucey, P.G., 2006. Spectral properties of angrites. *Meteorit. Planet. Sci.* 41, 1139–1146.
- Burbine, T.H., McCoy, T.J., Jarosewich, E., Sunshine, J.M., 2002. Spectral measurements of meteorite powders: Implications for 433 Eros. *Lunar Planet. Sci.* 33. Abstract 1359.
- Bus, S.J., Binzel, R.P., 2002. Phase II of the Small Main-Belt Asteroid Spectroscopic Survey: The observations. *Icarus* 158, 106–145.
- Clark, B.E., Hapke, B., Pieters, C., Britt, D., 2002a. Asteroid space weathering and regolith evolution. In: Bottke, W., Cellino, A., Paolicchi, P., Binzel, R.P. (Eds.), *Asteroids III*. Univ. of Arizona Press, Tucson, pp. 585–599.
- Clark, B.E., Helfenstein, P., Bell III, J.F., Peterson, C., Veverka, J., Izenberg, N.I., Domingue, D., Wellnitz, D., McFadden, L., 2002b. NEAR infrared spectrometer photometry of Asteroid 433 Eros. *Icarus* 155, 189–204.
- Clark, B.E., Bus, S.J., Rivkin, A.S., McConnochie, T., Sanders, J., Shah, S., Hiroi, T., Shepard, M., 2004. E-type asteroid spectroscopy and compositional modeling. *J. Geophys. Res. (Planets)* 109, doi:10.1029/2003JE002200.
- Cloutis, E.A., Gaffey, M.J., Jackowski, T.L., Reed, K.L., 1986. Calibrations of phase abundance, composition, and particle size distribution for olivine–orthopyroxene mixtures from reflectance spectra. *J. Geophys. Res.* 91, 11641–11653.
- Connors, M., Stacey, G., Brasser, R., Wiegert, P., 2005. A survey of orbits of co-orbitals of Mars. *Planet. Space Sci.* 53, 397–408.
- Delbó, M., Harris, A.W., Binzel, R.P., Pravec, P., Davies, J.K., 2003. Keck observations of near-Earth asteroids in the thermal infrared. *Icarus* 166, 116–130.
- Dixon, E.T., Bogard, D.D., Garrison, D.H., 2003. ³⁹Ar–⁴⁰Ar chronology of R chondrites. *Meteorit. Planet. Sci.* 38, 341–355.
- Gaffey, M.J., 1976. Spectral reflectance characteristics of the meteorite classes. *J. Geophys. Res.* 81, 905–920.
- Gaffey, M.J., Bell, J.F., Brown, R.H., Burbine, T.H., Piatek, J.L., Reed, K.L., Chaky, D.A., 1993. Mineralogical variations within the S-type asteroid class. *Icarus* 106, 573–602.
- Gendrin, A., Langevin, Y., Erard, S., 2005. ISM observation of Phobos reinvestigated: Identification of a mixture of olivine and low-calcium pyroxene. *J. Geophys. Res.* 110, doi:10.1029/2004JE002245.
- Gomes, R., Levison, H.F., Tsiganis, K., Morbidelli, A., 2005. Origin of the cataclysmic Late Heavy Bombardment period of the terrestrial planets. *Nature* 435, 466–469.
- Hinrichs, J.L., Lucey, P.G., 2002. Temperature-dependent near-infrared spectral properties of minerals, meteorites, and lunar soil. *Icarus* 155, 169–180.
- Kallemyn, G.W., Rubin, A.E., Wasson, J.T., 1996. The compositional classification of chondrites. VII. The R chondrite group. *Geochim. Cosmochim. Acta* 60, 2243–2256.
- Kurat, G., Varela, M.E., Brandstatter, F., Weckwerth, G., Clayton, R.N., Weber, H.W., Schultz, L., Wasch, E., Nazarov, M.A., 2004. D'Orbigny: A non-igneous angritic achondrite? *Geochim. Cosmochim. Acta* 68, 1901–1921.
- Landolt, A.U., 1983. UBVR photometric standard stars around the celestial equator. *Astron. J.* 88, 439–460.
- Marzari, F., Scholl, H., Murray, C., Lagerkvist, C., 2002. Origin and evolution of Trojan asteroids. In: Bottke, W., Cellino, A., Paolicchi, P., Binzel, R.P. (Eds.), *Asteroids III*. Univ. of Arizona Press, Tucson, pp. 273–287.
- McSween Jr., H.Y., Lauretta, D.S., Leshin, L.A., 2006. Recent advances in meteoritics and cosmochemistry. In: Lauretta Jr., D.S., McSween, H.Y. (Eds.), *Meteorites and the Early Solar System II*. Univ. of Arizona Press, Tucson, pp. 53–66.
- Morbidelli, A., Levison, H.F., Tsiganis, K., Gomes, R., 2005. Chaotic capture of Jupiter's Trojan asteroids in the early Solar System. *Nature* 435, 462–465.
- Moroz, L., Schade, U., Wäsch, R., 2000. Reflectance spectra of olivine–orthopyroxene-bearing assemblages at decreased temperatures: Implications for remote sensing of asteroids. *Icarus* 147, 79–93.
- Rayner, J.T., Toomey, D.W., Onaka, P.M., Denault, A.J., Stahlberger, W.E., Vacca, W.D., Cushing, M.C., Wang, S., 2003. SpeX: A medium-resolution 0.8–5.5 micron spectrograph and imager for the NASA Infrared Telescope Facility. *Publ. Astron. Soc. Pacific* 115, 362–382.
- Rivkin, A.S., Brown, R.H., Trilling, D.E., Bell, J.F., Plassmann, J.H., 2002. Infrared spectrophotometry of Phobos and Deimos. *Icarus* 156, 64–75.
- Rivkin, A.S., Binzel, R.P., Howell, E.S., Bus, S.J., Grier, J.A., 2003. Spectroscopy and photometry of Mars Trojans. *Icarus* 165, 349–354.
- Rivkin, A.S., Binzel, R.P., Sunshine, J., Bus, S.J., Burbine, T.H., Saxena, A., 2004. Infrared spectroscopic observations of 69230 Hermes: Possible unweathered end-member among ordinary chondrite analogs. *Icarus* 172, 408–414.
- Rubin, A.E., Mittlefehldt, D.W., 1993. Evolutionary history of the mesosiderite asteroid—A chronologic and petrologic synthesis. *Icarus* 101, 201–212.
- Scholl, H., Marzari, F., Tricarico, P., 2005. Dynamics of Mars Trojans. *Icarus* 175, 397–408.
- Singer, R.B., Roush, T.L., 1985. Effects of temperature on remotely sensed mineral absorption features. *J. Geophys. Res.* 90, 12434–12444.
- Sunshine, J.M., Bus, S.J., Burbine, T.H., McCoy, T.J., 2005. Tracing oxygen fugacity in asteroids and meteorites through olivine composition. *Lunar Planet. Sci.* 36. Abstract 1203.

- Tabachnik, S., Evans, N.W., 1999. Cartography for martian Trojans. *Astrophys. J.* 517, L63–L66.
- Tody, D., 1986. The IRAF data reduction and analysis system. In: Crawford, D.L. (Ed.), *Instrumentation in Astronomy VI*. In: *Proc. SPIE*, vol. 627. SPIE, Bellingham, WA, p. 733.
- Trilling, D.E., Rivkin, A.S., Stansberry, J.A., Spahr, T.B., Crudo, R.A., Davies, J.K., 2007. Albedos and diameters of three Mars Trojan asteroids. *Icarus* 192 (2), 442–447.
- Varela, M.E., Kurat, G., Zinner, E., Hoppe, P., Ntaflou, T., Nazarov, M.A., 2005. The non-igneous genesis of angrites: Support from trace element distribution between phases in D’Orbigny. *Meteorit. Planet. Sci.* 40, 409–430.
- Weisberg, M.K., McCoy, T.J., Krot, A.N., 2006. Systematics and evaluation of meteorite classification. In: Lauretta, D.S. Jr., McSween, H.Y. (Eds.), *Meteorites and the Early Solar System II*. Univ. of Arizona Press, Tucson, pp. 19–52.